Application of geoelectrical resistivity method for the assessment of shallow aquifer quality in landfill areas

Nur Islami · Mitri Irianti · Fakhruddin Fakhruddin · Azhar Azhar · Muhammad Nor

Abstract In this article, a valuable approach utilizing the relationship between select physical water and soil characteristics and geoelectrical resistivity data was used to recognize and trace groundwater contamination by using the geoelectrical resistivity data of a landfill area. It can reduce uncertainty in geoelectrical resistivity interpretation. By interpreting and calibrating the resistivity model with the lithology and physical characters of water samples, it was possible to identify the unique paths of landfill leachate that occurred throughout a shallow aquifer. The water physical property analysis showed that the landfill area was contaminated by a relatively high amount of total of dissolved solids (TDSs). A scatter plot of TDS values and directly measured resistivity showed that resistivity decreased with increasing TDSs. The movement direction of the landfill leachate in the aquifer system was clearly observed in a depth slice of the resistivity distribution. The aquifer is considered to be contaminated starting from the landfill zone and extending to the northeastern part of the study area.

N. Islami (✉) · M. Irianti · F. Fakhruddin · A. Azhar · M. Nor
Physics – PMIPA, FKIP, University of Riau, Pekanbaru, Riau 28293, Indonesia
e-mail: nurislami@lecturer.unri.ac.id

Introduction

Municipal solids are unwanted manufactured goods that have been used for certain activities. Municipal solid wastes comprise daily items that humans use, such as food, papers, packaging, clothing and bottles (Yunmei et al. 2017; Thitame et al. 2010). These waste products are generated from human activity and increase as the population of humans increases. These products are collected and sent to landfill disposal sites. The waste production percentage indicates the development of a country or a city. The generation of solid waste depends on several factors, such as the development of the country or city and the level of education and awareness of residents. The increase in waste generation has affected society and the environment. Furthermore, the amount of waste increases in parallel with industry activity. As a result, this type of activity has brought about an increase in waste generation and pollution (Rotich et al. 2006; Chiemchaisri et al. 2007).

Several investigations on the impacts of landfill leachates have been published. Among these investigations are reports that landfill leachate is a major source of trace organic pollutants, and the pollutants that can significantly affect the quality of the surrounding environment (Clarke et al. 2015). Negi et al. (2018) successfully used heavy metals and microbiological indicators to define the quality of an environment that has been impacted by landfill leachates. This study found that the contents of heavy metals and microbiology were relatively high and far above the recommended limits in groundwater (Negi et al. 2018). Landfill age has no role

in producing leachate. Young landfills also have the potential to produce leachate, with high leachate levels found in relatively new landfills (Brennan et al. 2016). In addition to landfill leachate, plastic disposal influences crop yield and has a large impact on land degradation (Haque et al. 2018).

Increasing urbanization in a city has apparent impacts on the groundwater in areas surrounding landfill sites (Wakode et al. 2018). The landfill leachate in developing countries threatens to pollute groundwater resources. Groundwater pollution by landfills can be assessed using the leachate pollution index combined with error estimation (Mor et al. 2018). The physicochemical parameters of toxic metals and microbiological parameters can also be employed to determine the contaminants released from municipal solid waste landfills (Samadder et al. 2017). In addition, water quality and sediment contamination can be assessed statistically using multivariate analysis of pollution indicators (Ustaoğlu and Tepe 2018).

The use of geophysical methods to study geoscience problems is supported by several advantages such as the relatively low operation costs and high data acquisition effectiveness of these methods. Furthermore, the results of geophysical methods can be obtained in a relatively short time, and they can be repeated many times over the same area at various time intervals. The geophysical method, particularly geoelectrical resistivity surveys, has been widely used in several geosciences and environmental studies. In these studies, the resistivity survey has been used to investigate how nitrate affects soil resistivity (Islami 2010). It has also been used to monitor the amount of nitrate in the soil so that the fate of nitrate can be determined with information about the initial soil condition and the amount of chemical fertilization (Islami et al. 2011). The presence of nitrate in shallow groundwater can also be assessed using geoelectrical resistivity (Islami et al. 2012). The geoelectrical resistivity method has been used to assess the intrusion of sea water in relation to sustainability agriculture in coastal areas (Göktürkler et al. 2008; Baharuddin et al. 2013; Kaya et al. 2015). The occurrence of heavy metals in aquifers can lead to groundwater contamination (Haihai et al. 2018). A geoelectrical resistivity survey was successfully used to delineate and map the heavy metal zones in aquifer systems (Islami et al. 2018). Geoelectrical methods have been used not only in groundwater research but also to predict the yields of two types of yams and grain size (Akanji et al. 2018).

This paper investigated the leachate in groundwater caused by open landfills using geoelectrical resistivity and soil and water physical analysis methods. We propose the utilization of the relationship between soil and groundwater characteristics with geoelectrical resistivity to investigate the possible pollution impact of open landfills on shallow aquifers. Thus, the possibility of groundwater pollution around a landfill can be recognized and traced in an undirect way using geoelectrical resistivity data.

Materials and methods

Study area

The location of this study is an open landfill site in Pekanbaru, Sumatera Island, Indonesia. The area of the landfill is approximately 5 ha and is surrounded by a palm oil plantation area. It is estimated that approximately 170 m^3 of garbage are sent to this landfill every day. Geologically, the landfill is composed of quaternary sediments that have not been consolidated. Generally, these sediments are part of the central Sumatran basin (Roger et al. 1981). The soil composition in landfills and surrounding areas are dominated by sand, silt, clay and mixtures thereof. The elevation of the study area varies from 35 to 63 m above mean sea level (a.m.s.l). The garbage disposal zone is located on the slope of the valley. Figure 1 shows the location of the study area taken from Google Earth. The yellow line in the figure is the path of the resistivity survey, and the white dot is the location of the water sample.

Survey

Several methods were used in this study. In the field, water samples were collected to obtain the physical characteristics of the water throughout the landfill and surrounding area. Then, the resistivity of the soil was correlated with the fluid characteristics in the study area. Finally, 2D resistivity surveys were conducted. These integrated methods were needed due to the resistivity of the soil is affected by several factors, the grain size of sand matrix and the water content of the pore soil (Telford et al. 1990; Islami 2010).
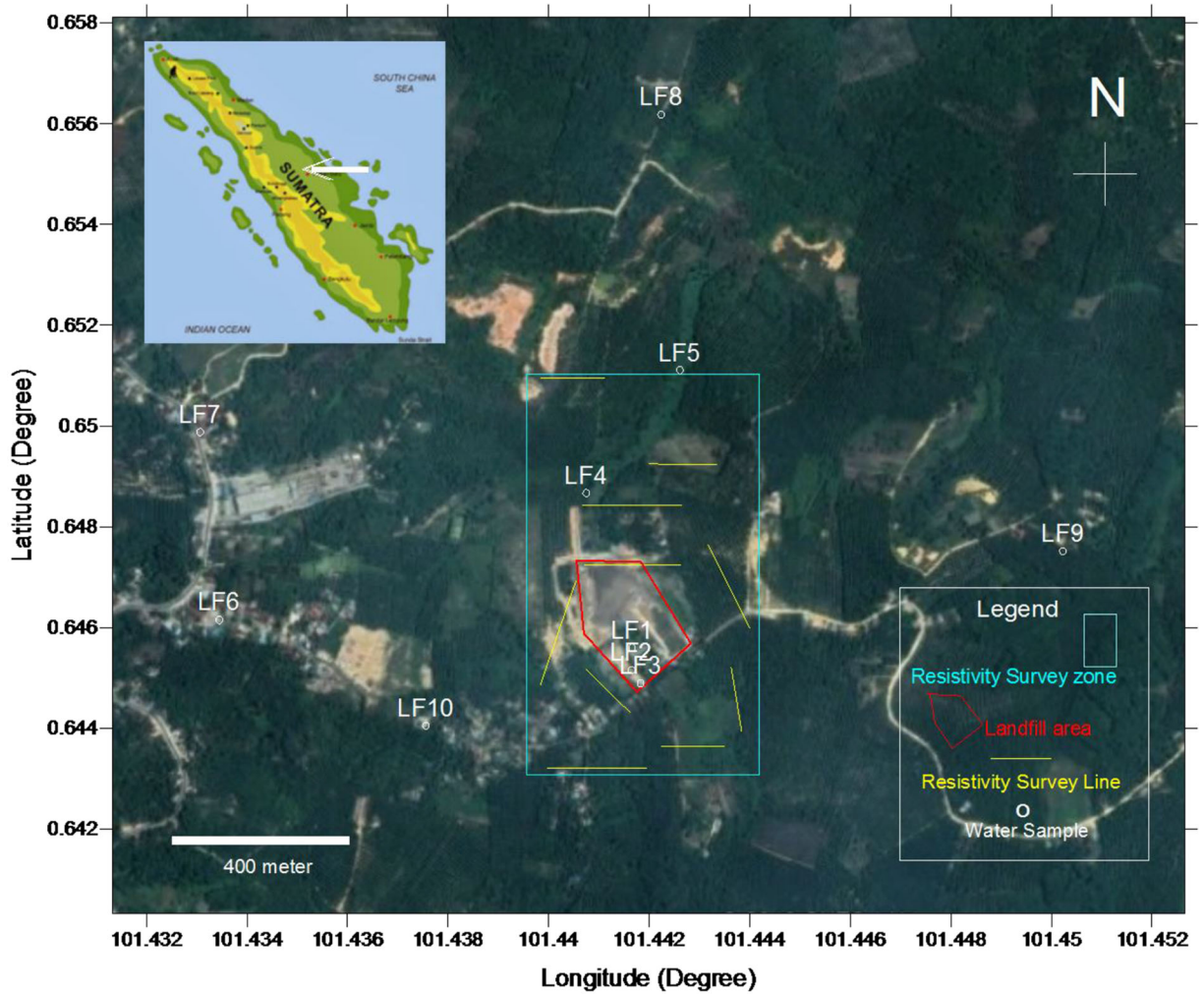
Fig. 1 The location and situation of the study area. In the map, the *X* and *Y* axes show longitude and latitude, respectively

Soil characterisation

Soil samples were taken from several sites where the resistivity survey was conducted, including the newly drilled wells. The soil grain size and moisture content were analysed. Grain size and moisture content data have an important role in generating geoelectrical resistivity readings, which higher moisture content will

reduce the resistivity value, whilst higher sand grain size raises the resistivity value (Telford et al. 1990). The analysis of grain size was performed using mechanical sieves manufactured by Wykeham Farrance; the soil samples were grouped into clay, silt, sand and gravel (Barnes 2016). The moisture content of the soil sample was measured using the gravimetric method, i.e. moisture was determined from the weight reduction of the soil before and after drying (Black 1965).

Physical water quality

Water samples were taken from surface waters, such as ponds and small drainage areas, at locations in the study area. In situ physical parameters of the water samples, such as conductivity, salinity, total dissolved solids (TDSs) and temperature, were measured using EC300 YSI precision equipment immediately after sampling. The resistivity value of the water sample was measured using a resistivity meter. The in situ physical parameters of the water samples were measured five times for each water sample to control the quality measurement. The retrieval of groundwater samples was performed at existing wells in the community and at newly drilled wells.

Geoelectrical resistivity

Resistivity data can be obtained from the measurement of the voltage difference (V) between two electrodes P1 and P2 and the measurement of the current (I) injected at electrode C1 that exits at electrode C2 (Fig. 2).

To produce an apparent resistivity data point, an electric current (I) is injected at C1 (source) and will exit at C2 (sink). Thus, the voltage at P1 or P2 can be calculated as follows:

$$V_P = V_{\text{source}} - V_{\text{sink}} = \frac{I\rho}{2\pi}\left(\frac{1}{r_{\text{source}}} - \frac{1}{r_{\text{sink}}}\right)$$

where r_{source} is the distance from C_1 to P_1 or the distance from C_1 to P_2, and r_{sink} is the distance from
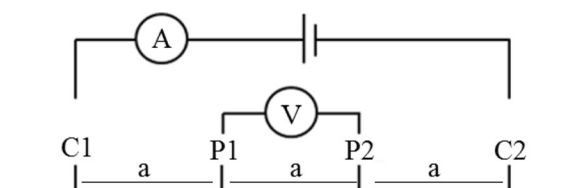
Fig. 2 Electrode arrangement

C_2 to P_1 or to P_2. Thus, the voltage difference at P_1 and P_2 fulfils the following equation:

$$\Delta V = V_{P1} - V_{P2} = \frac{I\rho}{2\pi}\left(\frac{1}{r_1} - \frac{1}{r_2} - \frac{1}{r_3} + \frac{1}{r_4}\right)$$

where r_1 is the distance from P_1 to C_1, r_2 is the distance from P_1 to C_2, r_3 is the distance from P_2 to C_1, and r_4 is the distance from P_2 to C_2.

For the Wenner configuration, the distance for each electrode is a; then, apparent resistivity (ρ) can be obtained using:

$$\rho = 2\pi a \frac{\Delta V}{I}$$

In the above equation, ΔV and I can be measured directly using a voltmeter and ampere metre, and a is the distance for each electrode (Telford et al. 1990; Balkaya et al. 2009).

For the purposes of 2D resistivity data interpretation, in this study, some direct resistivity measurements were carried out using a Wenner configuration with electrodes separated by 3 cm; at this small distance, the earth material is assumed to be homogeneous. The results of the measurements were used to obtain the true resistivity values for certain materials under specific conditions. In a survey with a small electrode spacing, the apparent resistivity becomes the true resistivity of the material, assuming that the material is homogeneous (Telford et al. 1990). This measurement is a direct way to obtain the correlation between the resistivity and the fluid content in the pores of the soil.

In the present research, a 2D geoelectrical resistivity survey was conducted using in-house-made resistivity meter equipment. The equipment could generate an optional output current of 100 mA, 250 mA and 500 mA. The choice of current was adjusted based on the need in the field. A total of ten survey lines were conducted on October 2018. For each profile, 40 electrodes were separated by varying distances (3 to 5 m apart) depending on the available space in the field. Besides, the target depth penetration was a shallow aquifer with depth less than 15 m. In order to cover the shallow aquifer, the longest stretch of electrode was adjusted 200 m length with the total of 40 electrodes and resulted 30 m depth in the inversion model.

The Wenner configuration was employed for the whole survey because this configuration has a higher signal strength than other configurations and provides

relatively high vertical resolution (Telford et al. 1990). A total of 12 layers of measurements produced 246 apparent resistivity data points for each resistivity survey line, as indicated in Fig. 3. For the first layer ($n = 1$), the electrode spacing was a, and for the next multifaction of n, the electrode spacing was increased proportional to the increment of n (example: for $n = 2$, so a will be $2a$). The raw field data obtained from each survey were processed using the inversion software RES2DINV (Loke 2004), which provided an inverse model of the true resistivity profile. The model was approximated as an actual subsurface resistivity distribution (Loke and Barker 1996). Topography data at each electrode was included in the geoelectrical resistivity inversion process which used the distorted finite-element grid with uniform distortion. This method gives more accurate results among the other methods which is in this inversion, the nodes below the surface (and thus also the model layers) are shifted to the same extent as the surface nodes (Loke 2000).

Results

Soil distribution

Table 1 shows the soil grain size distribution at wells LF4 and LF5. In addition to obtaining the soil grain size distribution with depth, these wells provided physical water characteristic data that were used to determine the quality of groundwater and were correlated with the resistivity data. For both wells (LF4 and LF5), silt and clay are dominant at the near surface. They decrease with depth until the maximum depth of the well. The content of silt and clay at the near surface is higher in LF5 than in LF4 because LF5 is surrounded by a relatively highly undulating ground. The content of fine sand increases from the surface to a depth of 23 m a.m.s.l. The content of medium-sized sand increases drastically at a depth of 29 m a.m.s.l. Based on the soil grain size, shallow aquifers are possible at a depth of 30 m downward; in this zone, sand is dominant compared to silt and clay. Generally, both wells have the same grain size distribution and the same grain size trend with depth.

In the other location, the soil sample was collected at the site where the resistivity survey was conducted. Figure 4 shows the silt and clay distribution and the sand distribution at the ground surface. In the figure, silt and clay are dominant at lower ground elevations due to the impact of transportation by rain water. The observed sand grain size demonstrates the opposite conditions with silt and clay.

Physical water quality

The water sample results are given in Table 2. Physical parameters, namely conductivity (μS/cm), total dissolved solids (mg/l), pH, and salinity (ppt%), were tested in the field directly just after the water sample was obtained.

The water samples in this research were obtained from ponds, wells, drainage systems, and two new wells. At the studied landfill, there are three ponds that were installed by the government. These ponds are used for the normal landfill treatment procedure in the area. The water sample locations are presented as the degree of latitude and longitude. The depth to the water table was measured from the ground surface surrounding the water table. As shown in Table 2, the conductivity values ranged from 91 to 770 μS/cm. The difference between the lowest and the highest values was quite large for the covered area. The highest value was obtained from pond 3 (LF3), which may be because pond 3 is the first gathering leachate zone of raw garbage. The lowest value (91 μS/cm) of conductivity was obtained from well LF6, which is located approximately 1000 m west of the landfill. For the other wells, which are located in the northwest (LF7), southwest (LF10), and east (LF9) of the landfill (Fig. 1), the water sample conductivity values were 96, 98, and 115 μS/cm, respectively. Because there was no existing well in the northern part of the landfill area, in this study, two new wells were drilled using a hand auger 2 in in diameter. The conductivity values of the new wells (562 and 261 μS/cm) were higher than those of other existing wells.

The TDS value ranges from 121 to 1861 mg/L (Table 2); TDS values that are suitable for human consumption are less than 300 mg/L (WHO, 1996). The highest value was at LF3 (1861 mg/L), whilst the TDS values of the other ponds were higher than those of the other water samples. Figure 5 shows a scatter plot between TDSs and conductivity. The line in the scatter plot (TDSs vs conductivity) indicates the trend between TDSs and conductivity. TDSs and conductivity have a positive correlation, with conductivity increasing with TDSs. An R^2 of 0.9862 is the correlation between the two variables, which indicates that the amount of TDSs
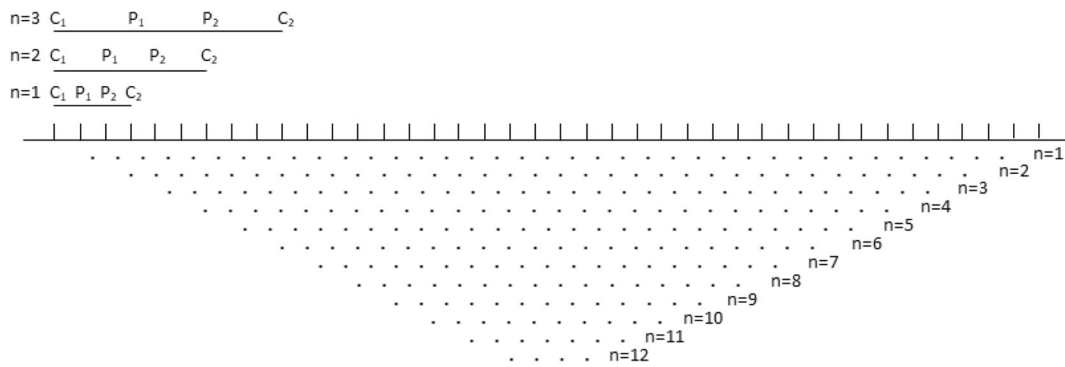
Fig. 3 The data acquisition design for each geoelectrical resistivity survey

has an impact on the ability to transfer electric current through the pore fluid in the soil. In Fig. 5, furthermore, there are three groups of data coloured red, orange and green. The three groups have different values of TDSs and conductivity. The red group was obtained from ponds, and the orange group was obtained from the drainage area and two wells in the north. The water samples of the green group were obtained from the wells in the west and east.

The pH and salinity of the water sample demonstrate no good correlation with TDSs and conductivity. The last physical character is resistivity. In this research, the resistivity values of water samples were obtained from direct measurements. The resistivity value was the highest when the TDS value was high, and resistivity was low in samples with lower TDS values.

The physical parameters of the water varied according to the distance and direction from the landfill. The

zones that have been contaminated by landfill material definitely show different values compared to other locations that have not been contaminated. For example, the TDS value was the highest in pond 3, where landfill leachates gather. This proves that in the landfill, the water samples were concentrated, with higher dissolved ion concentrations, and were definitely contaminated. However, the type of contaminant was not investigated in this study because contamination can vary among materials. On the other hand, the lowest value of TDS (161 mg/L) was observed at LF6, which is approximately 1000 m to the west. As shown in the map (Fig. 1), the amount of TDSs was very low in LF6 compared to LF1, LF2, and LF3. This means that the lower TDS zone to the west and the east of the landfill were not contaminated by the leachate released from the landfill. As shown in the topographic map, the landfill is located between two high-elevation zones, and a valley is to the

Table 1 Soil grain size distribution at the well LF4 and LF5

ID	Depth m (a.m.s.l)	Gravel (%)	Coarse sand (%)	Med sand (%)	Fine sand (%)	Silt and clay (%)	Moisture (%)
LF4	38	0	0	7.02	19.4	73.58	5.22
	35	0	0	9.04	20.82	70.14	11.54
	32	0	0	10.52	24.87	64.61	38.15
	29	0	4.51	29.03	27.28	39.18	Fully saturated
	26	0	8.13	35.01	32.64	24.22	Fully saturated
	23	0	9.25	40.98	34.21	15.56	Fully saturated
LF5	38	0	0	2.02	17.66	80.32	5.82
	35	0	0	8.12	18.46	73.42	11.04
	32	0	0	10.12	23.64	66.24	38.07
	29	0	4.38	29.18	26.42	40.02	Fully saturated
	26	0	8.08	35.52	32.24	24.16	Fully saturated
	23	0	9.02	41.25	33.21	16.52	Fully saturated
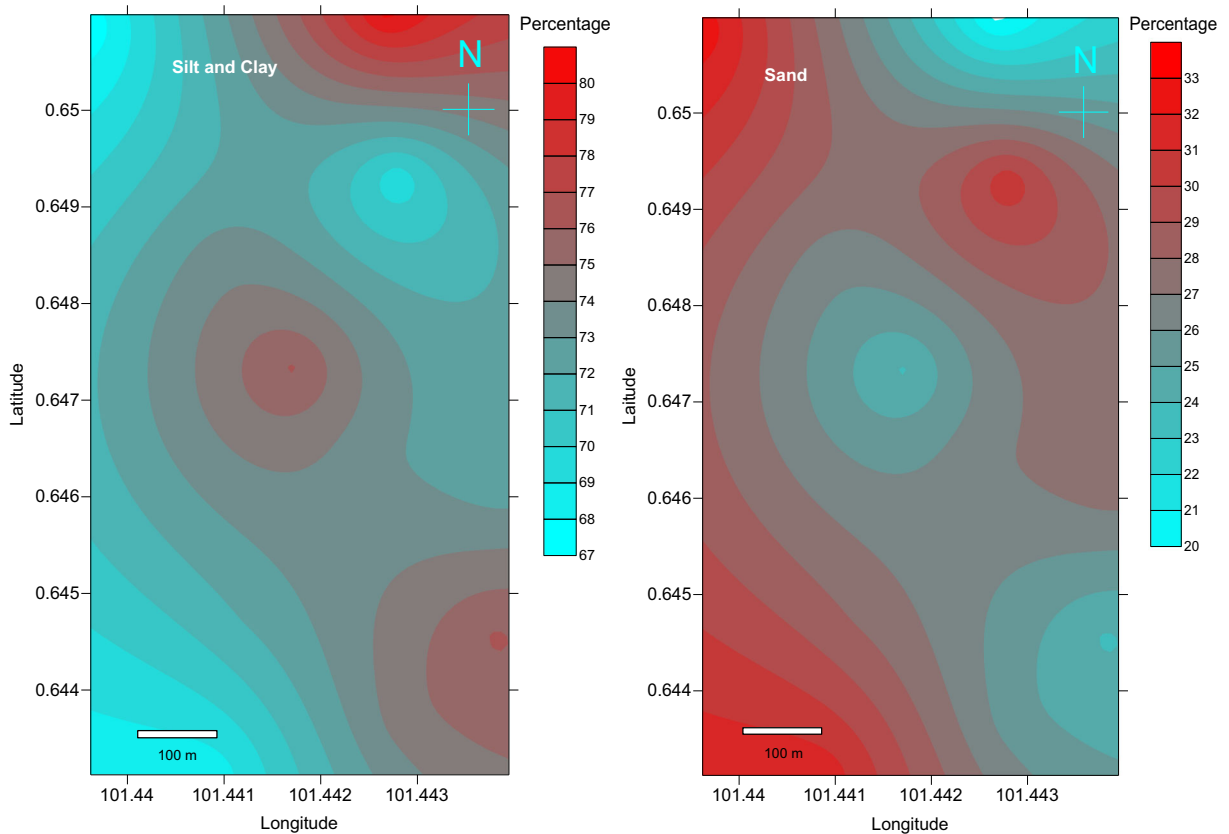
Fig. 4 Soil grain size distribution on the surface

north. These factors prevent the leachate from flowing to the west and east.

The best way to find the relationship between TDSs and the resistivity of a water sample is to use a cross plot of both parameters. Figure 6 shows the scatter plot of TDSs and resistivity. In the figure, the amount of TDSs is almost directly proportional to resistivity. A high amount of TDSs means that the amount of dissolved ions in the water is also high, which will enable the flow of the electric current and thus lower the resistivity value of the water sample. This result indicates that a small amount of ions in fluid can reduce the resistivity value drastically.

Groundwater flow

Figure 7 shows the groundwater levels obtained from the existing wells (LF6, LF7, LF9, and LF10) and the newly drilled wells (LF4, LF5). The contour was obtained from the measurement of the reduction between the ground surface and water table depth. The groundwater level contour was produced using Kriging method

which is used to estimate the value of a point or block as a linear combination of the sample values that are around the point to be estimated. In Fig. 7, the groundwater level is relatively high in the southern part of the area and gradually decreases northward. Based on the contour in Fig. 7, generally, the groundwater flows from the south to the north.

Geoelectrical resistivity correlation

Calibration data are very important in geoelectrical resistivity studies. The calibration data were obtained from direct resistivity measurements on ground materials. The direct resistivity measurement method using a small electrode spacing was employed; thus, it could be assumed that the materials were homogenous. As a result, the measured apparent resistivity became the true resistivity of the material (Telford et al. 1990). Once obtained, the true resistivity can be correlated to the quality of the water in the soil pores, as well as the soil characteristics. The resistivity values obtained from this measurement were used for the interpretation of the

Table 2 Physical properties of the water sample

No	Samp. ID	Long. (°)	Latitude (°)	Source	Elev. (m)	Depth to water (m)	Conduct. (μS/cm) and Stdv	TDSs (mg/l) and Stdv	pH and stdv	Salinity (ppt%) and Stdv	Resist. direct measurement (Ohm m) and Stdev
1	LF1	101.44166	0.645598	Pond	53	0	746.3 (12.1)	1705.1 (14.2)	6.01 (0.02)	0.2 (0)	13.4 (0.2)
2	LF2	101.44165	0.645155	Pond	53	0	765.9 (11.3)	1749.4 (15.1)	6.08 (0.01)	0.2 (0)	13 (0.3)
3	LF3	101.44183	0.644894	Pond	53	0	770.2 (12.5)	1820.8 (14.6)	6.19 (0.02)	0.3 (0)	10.9 (0.3)
4	LF4	101.44075	0.648670	New Well 1	38	2.1	562.4 (9.8)	1081.3 (11.7)	6.01 (0.01)	0.2 (0)	21.1 (0.5)
5	LF5	101.44261	0.651162	New Well 2	42	6.2	260.8 (8.4)	688.4 (10.9)	6.21 (0.01)	0.1 (0)	38.4 (0.6)
6	LF6	101.43345	0.646152	Well	60	17.9	378.1 (11.1)	758.8 (12.6)	5.92 (0.01)	0 (0)	36.1 (1.1)
7	LF7	101.43307	0.649878	Well	58	16	91.3 (3.2)	161.1 (4.1)	6.08 (0.02)	0 (0)	109.8 (2.2)
8	LF8	101.44224	0.656185	Drainage	36	0	95.9 (6.2)	162.3 (4.4)	6.08 (0.01)	0.1 (0)	104.5 (1.8)
9	LF9	101.45023	0.647516	Well	48	6.5	115.2 (4.1)	214.0 (3.9)	6.05 (0.01)	0 (0)	87.4 (0.9)
10	LF10	101.43756	0.644048	Well	55	12	98.2 (3.2)	164.2 (3.7)	6.03 (0.01)	0 (0)	107.5 (1.1)

geoelectrical resistivity profile. Table 3 shows the resistivity values obtained via direct measurements for different soil conditions, as well as the correlation between these values and the water content. In Table 3, leachate-saturated soil has an average value of 18.3 ohm m., whilst the soil with contaminated water has an average value of 32.8 ohm m. The soil fully saturated by fresh water has a value of 128.6 ohm m, and the wet soil (with uncontaminated water) has a value of 374.2 ohm m. The highest average value, i.e. approximately 2101.6 ohm m, was observed in dry soil. In this study, the attention is emphasized at the leachate and contaminated water. Other direct resistivity measurements were also performed on the water sample, as shown in Table 1. Finally, to facilitate the interpretation of geoelectrical resistivity, the resistivity values in the profile were grouped on the colour scale, as shown in Fig. 9.

Geoelectrical resistivity results

Figure 8 shows the location of the geoelectrical resistivity survey and the topography map of the survey area. The dashed line in the map indicates the zone of the landfill.

In this study, the resistivity values of all resistivity models were adjusted to the same scale so that each contour colour in the resistivity model implies the same resistivity value. The range of resistivity for each possible material is marked in the resistivity scale (Fig. 9). The resistivity scale facilitates the interpretation of the geoelectrical resistivity model with respect to the direct resistivity measurement data.

The geoelectrical resistivity models of the survey area are given in Fig. 10. Interpretation of the resistivity models was based on the direct resistivity measurement data in Table 3. In the resistivity model, the resistivity value was grouped into 5 different resistivity ranges, as shown in Fig. 9. The different resistivity values represented different materials, including soil, groundwater, and leachate. Most of the geoelectrical resistivity survey sites were covered by dray sand and clay, especially on the areas of peak ground elevation. This will result in a relatively high resistivity value because the moisture in the material also plays an important role in the resulting resistivity.

Line 1 was located 200 m north of the landfill with an average elevation of 63 m a.m.s.l. The resistivity value of line 1 was approximately 2000 ohm m on the surface, which correlates to the dry soil conditions. The

Fig. 5 Cross plot of TDSs and conductivity
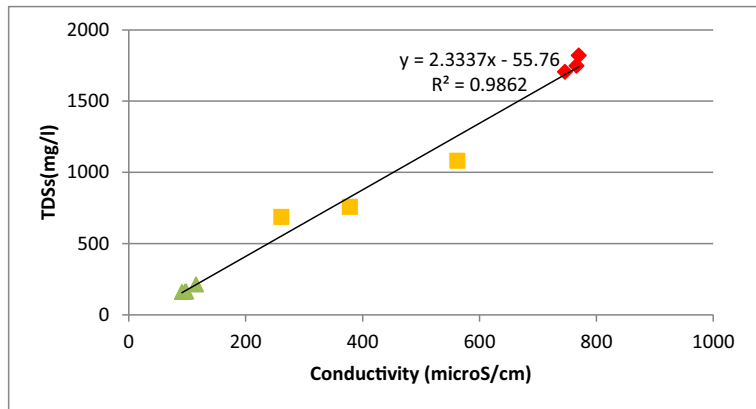
resistivity value did not change much with depth. At a depth of approximately 35 m a.m.s.l, the resistivity value still did not indicate the occurrence of water.

Line 2 was located approximately 50 m to the west of the landfill. In Line 2, the resistivity value was relatively low in the northwest. The resistivity value ranged from approximately 10–40 ohm m at a depth of 45 m downward, which indicated the presence of leachate in the zone. This means that leachate has contaminated the ground surface (0–24 m mark) soil and is seeping downward. In the field, when the survey was conducted, the ground surface was clearly contaminated by garbage at the 0–24 m mark. In the subsurface, the low resistivity zone was relatively flat, sloping towards the southeast. Below the 96 m mark, the resistivity value was relatively high, as found in line 1.

Line 3 was located 300 m to the southeast of the landfill. In line 3, the observed resistivity value was relatively high, and the resistivity model found no indication of leachate. The resistivity model of line 4 is located in the southeast part of the landfill. The nearest electrode from the landfill is at the 0 mark

approximately 150 m from the landfill. Line 4 stretched to the south and showed a relatively high resistivity value in general. However, at a depth of 35 m a.m.s.l, a low resistivity value zone showed a value of approximately 15 ohm m, which indicates the occurrence of leachate in the shallow aquifer.

Line 5 was located in the northern part of the landfill and was approximately 40 m from the landfill. The elevation of the first half of line 5 was 38–40 m a.m.s.l, and after the 100 m mark, the elevation increased to 40–45 m a.m.s.l. In line 5, the resistivity model was dominated by low resistivity values. Mostly, the resistivity model zone showed a resistivity value of less than 40 ohm m (coloured blue), which indicates that the soil had been contaminated landfill leachate. Leachate contaminated the surface soil and the shallow aquifer in this zone.

Line 6 was located in the northeast part of the landfill. The lowest elevation of the ground was 52 m at the last electrode and increased to 60 m at the first electrode. The resistivity model of line 6 was dominated by high resistivity values of more than 2000 ohm m. This means

Fig. 6 Cross plot of resistivity and TDSs
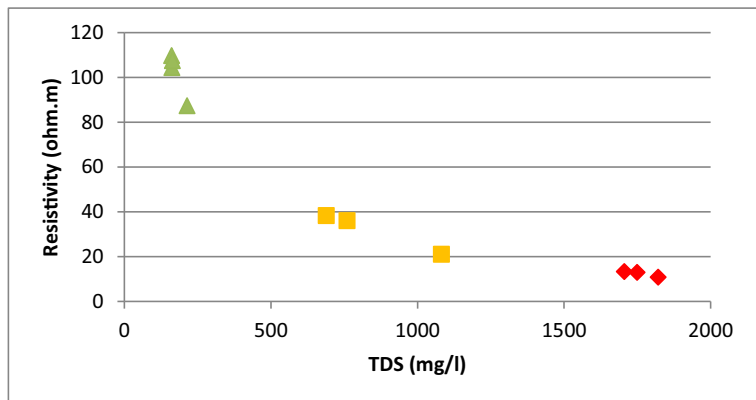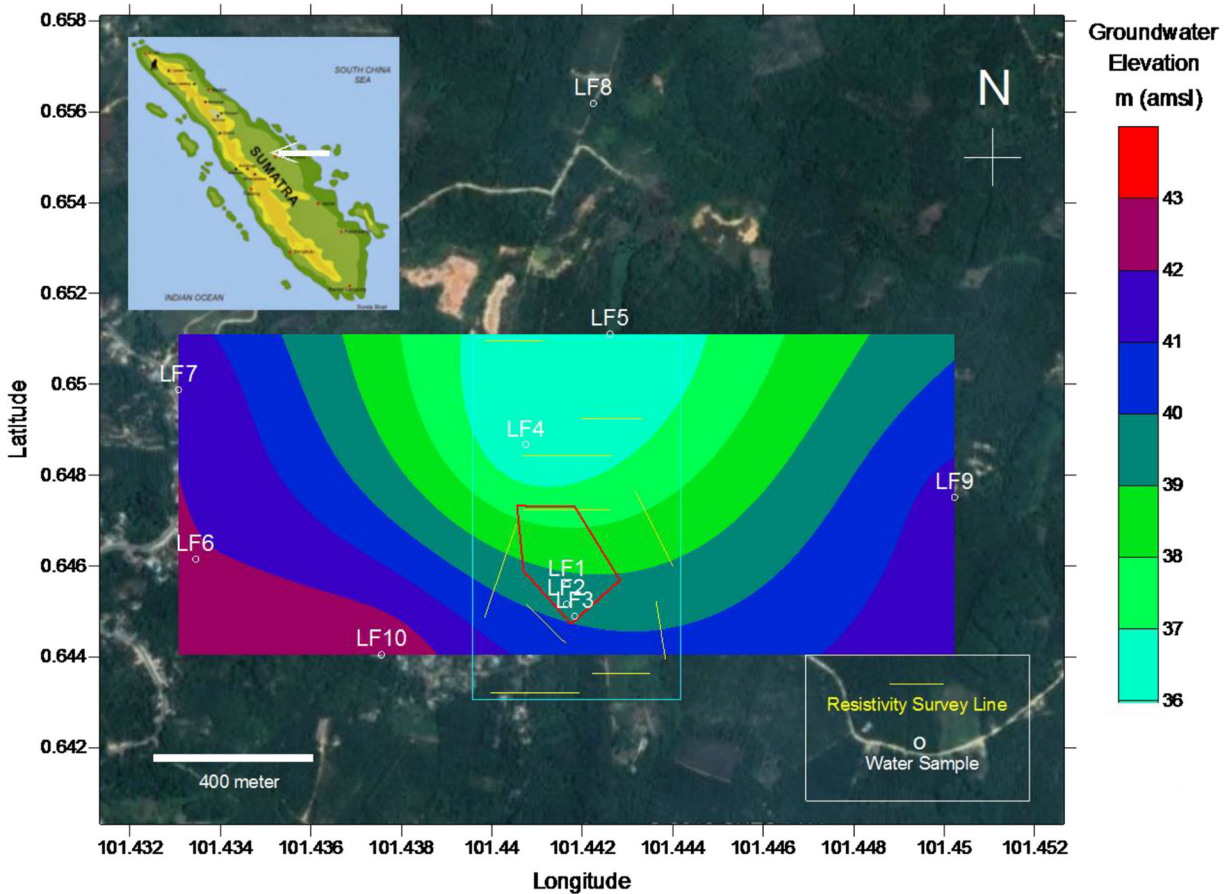
Fig. 7 Groundwater level obtained from the existing wells and two new wells

that the soil in the northeast was not contaminated by the landfill leachate.

The resistivity survey of line 7 was conducted west of the landfill. The first half of the electrode pair was initially placed in the high-elevation zone far away from the landfill and then was gradually moved to the landfill until the last electrode placement. The second half of the electrode pair was placed in the leachate-contaminated zone. This is indicated by the lower resistivity value (less than 20 ohm m) found on the surface. In the

subsurface, the blue colour of the resistivity value indicates leachate occurrence. However, in the southwest, the resistivity value drastically increased to more than 2000 ohm m. Based on line 7, the interface between the leachate and the uncontaminated zone can be clearly observed.

Line 8 was situated approximately 150 m after line 5 on the north side of the study site. At the ground surface, the resistivity value was higher than 900 ohm m. However, at a depth of 30 m downward, the resistivity value

Table 3 Resistivity values of materials

| Material	Number of samples	Resistivity range (Ωm)	Average resistivity (Ωm)
Leachate-saturated soil	6	10.9–31.6	18.3
Soil with contaminated water/fresh garbage	10	20.4–75.2	32.8
Freshwater-saturated soil	4	90.8–167.3	128.6
Wet soil (uncontaminated)	12	180.2–1453.3	374.2
Dry soil	12	1372.4–3870.1	2101.6
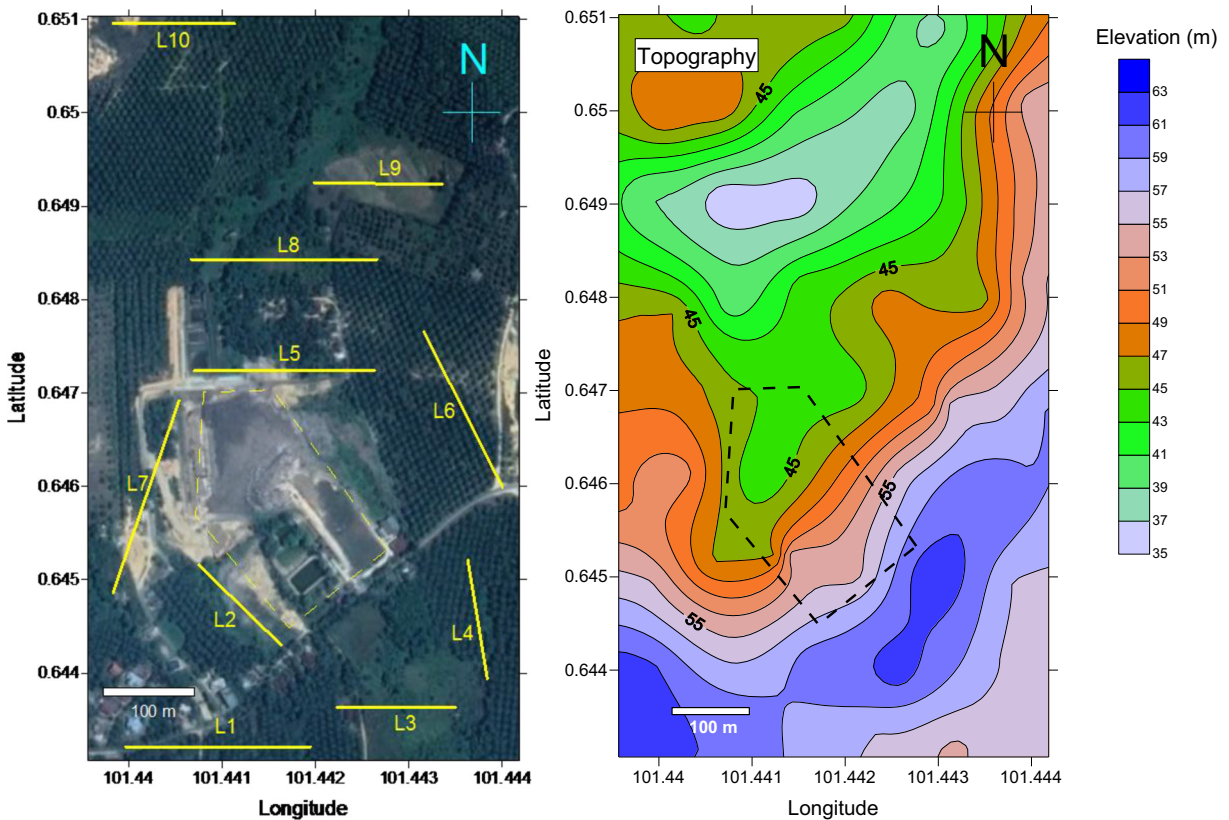
Fig. 8 Location and topography map of the geoelectrical resistivity survey

drastically changed to less than 30 ohm m. The lower resistivity value at this depth clearly indicates the occurrence of leachate from the landfill zone. The next line is line 9, which was located approximately 100 m to the north of line 8. In the resistivity profile of line 9, the resistivity at the subsurface was relatively low, with a value of approximately 40 ohm m. This value (approximately 40 ohm m) was higher than the value in line 8 (less than 30 ohm m). This result indicates that the concentration of the landfill leachate decreased with increasing distance from the landfill. The last survey was line 10, which was located 300 m from line 9 to the northwest. In the resistivity profile of line 10, it is obvious that the average resistivity value was higher than the resistivity value of Line 9. This means that in the subsurface at the zone of line 10, the shallow aquifer

was relatively uncontaminated by the landfill leachate. The resistivity value at the same depth in line 8 indicates that the aquifer was almost saturated by fresh water.

In general, the presence of landfill leachate in the subsurface can be identified in lines 2, 4, 5, 7, 8, 9 and 10. The location of these lines is clearly shown in Fig. 1. They are located immediately beside the landfill (lines 2, 4 and 7) and to the north of the landfill (5, 8, 9 and 10). Based on the resistivity profile, most of the lines in which landfill leachate was detected are concentrated on the north side of the study area. However, on the other sides (south, west and east), the resistivity profiles do not show any possibility of landfill leachate in the subsurface. The topographic map given in Fig. 8 shows that the ground surface at the northern part of the landfill has a relatively low

Fig. 9 Calibrated colour scale showing the resistivity range of materials and its condition
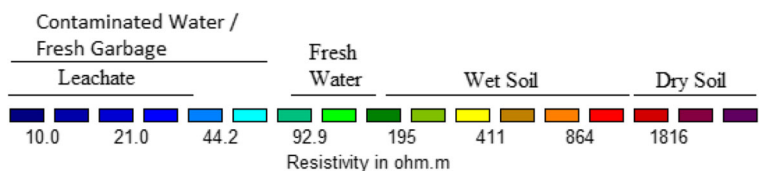
elevation on average when compared to the south part of the landfill. Although the landfill is barred by the concrete, when rain occurs, the leachate spills with the rain water from the fresh garbage and from the ponds. Furthermore, the landfill leachate seeps to the shallow aquifer and migrates farther to the northern part of the landfill.

Discussion

Figure 11 shows the depth slice of the true resistivity value. These depth slice maps were generated from the isoresistivity values obtained from each resistivity survey and mapped at the surface and at a certain depth (45, 35 and 25 m a.m.s.l). However, the total sample data in
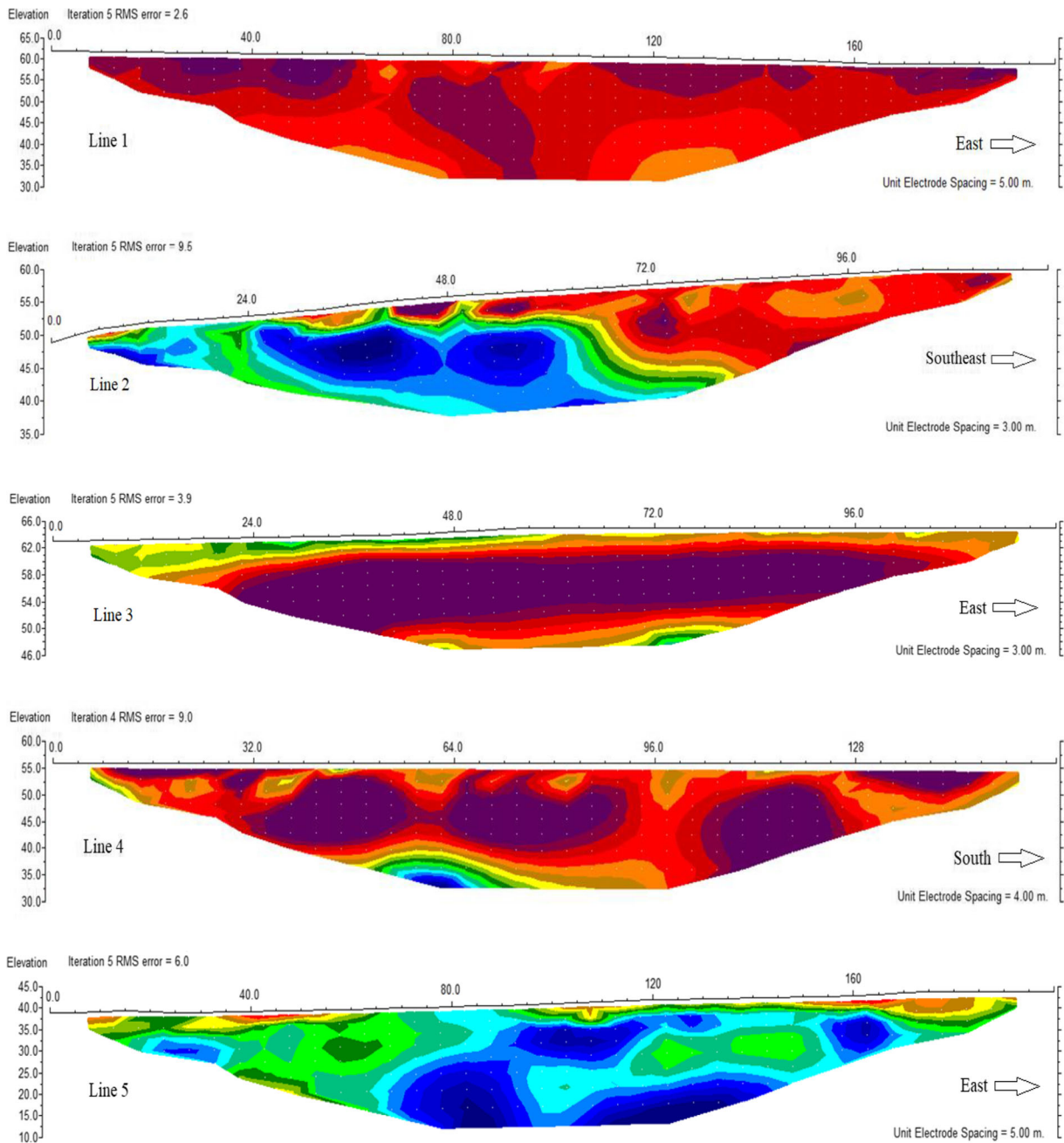
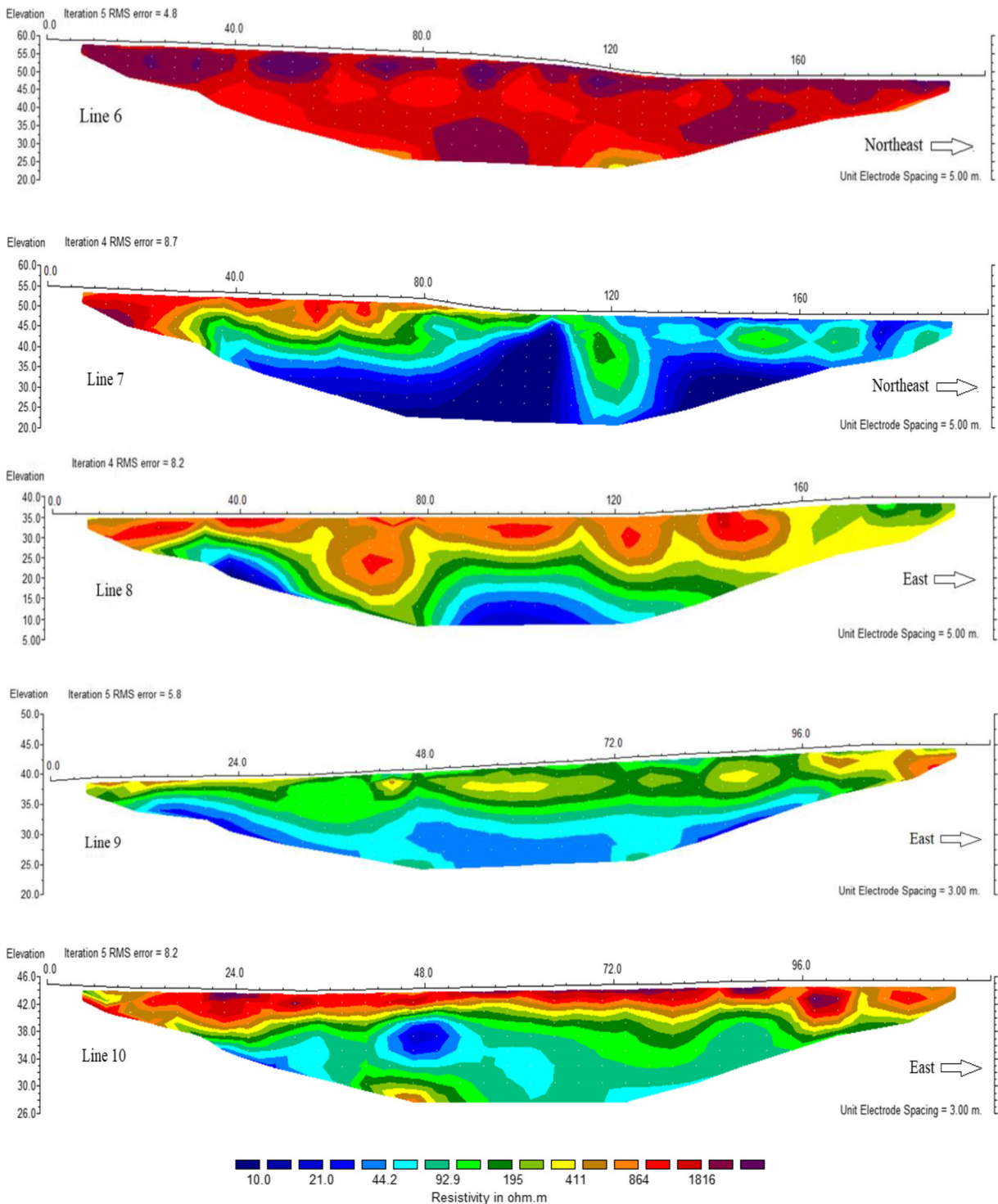Fig. 10 Geoelectrical resistivity model

Fig. 10 (continued)

the deeper depth (45 m a.m.s.l) will be less than in the near surface depth slice (25 m a.m.s.l) as shown in the resistivity model (Fig. 10). In Fig. 11, the gridding process is bounded by the rectangle indicated in Fig. 1 to produce reliable contour data. Generally, the resistivity depth slice in Fig. 11 shows a vast range of resistivity
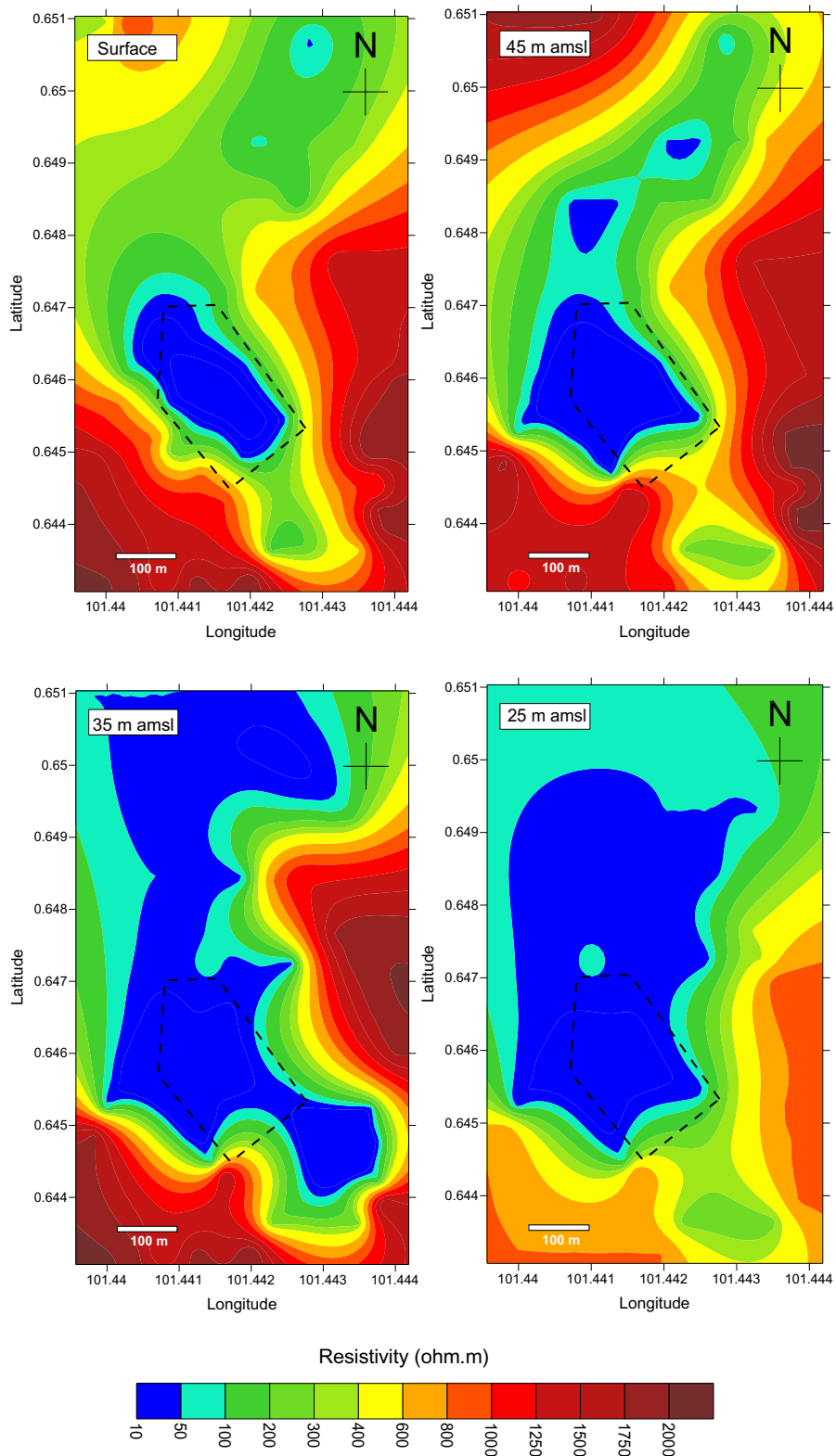
Fig. 11 Depth slice of the true resistivity value

values to indicate the distribution of the landfill leachate possibility. Based on the depth slices of resistivity, a relatively low resistivity value is observed on the surface just at the landfill. In the other parts of the study area, the resistivity value is relatively high, especially at the peak ground elevation. The relatively higher resistivity value at these zones is also confirmed by relatively higher content of sand size at these zones (Fig. 4). In the valley zone, the resistivity value is relatively low because the moisture content in the soil is relatively high. At a depth of 45 m a.m.s.l., the leachate moved to the northern part of the study area. The leachate was more concentrated at a depth of 35 m a.m.s.l than at other depths. The leachate also extends approximately 50 m to the southeast from the landfill. However, the landfill leachate extends less far at the depth of 25 m a.m.s.l than at the depth of 35 m a.m.s.l. This may be because the shallow aquifer does not reach this depth.

To verify what happened at the low resistivity zone in the northern part of the landfill zone, two new wells were drilled to a certain target depth. Well LF4 was drilled just after line 8, and the well was located in the low-resistivity zone in the geoelectrical model (line 8). The second well, LF5, was drilled at line 10, where the average resistivity value at the same depth was higher than the average resistivity value of line 8. In well LF4, the TDS value was relatively high (1081 mg/l) in the water sample, whilst the resistivity value at the depth 25 m was approximately 20 ohm m. In well LF5, the amount of TDSs (688 mg/l) was lower than the amount of TDSs in LF4, whilst the resistivity in the zone was approximately 55 ohm m. This proves that the TDSs in the groundwater reduce the resistivity of the aquifer. Based on this fact, the TDS value decreases with distance from the landfill. This is due to the soil surrounding the landfill; along the leachate pathway, this soil filtered the landfill leachate in the groundwater flowing from the landfill area.

Conclusions

In this research, the geoelectrical resistivity method was successfully used to investigate the zone landfill leachate migration zone in a shallow aquifer. The interpretation of the geoelectrical resistivity profile was integrated with the physical character of the groundwater sample and direct resistivity measurement of certain soil conditions. The correlation of the physical character of the water sample with the resistivity value was key in the interpretation of geoelectrical resistivity data. The in situ physical parameters of the water samples in the study area show that some water samples have been contaminated by leachate. The possibility aquifer contamination was clearly shown by the geoelectrical resistivity model, and the interpretation was enhanced with a direct resistivity measurement of earth material. Low resistivity values were correlated with soil contaminated by leachate. To make it easier to analyse the leachate pathway and the possibility that a zone was contaminated by landfill leachate, a depth slice of resistivity values was made at a certain depth. It was clearly shown that landfill leachates moved from the landfill zone towards the north in the depth range of the shallow aquifer zones in this area.

References

Akanji, M. A., Oshunsanya, S. O., & Alomran, A. (2018). Electrical conductivity method for predicting yields of two yam (Dioscorea alata) cultivars in a coarse textured soil. *International Soil and Water Conservation Research, 6*(3), 230–236.

Baharuddin, M. F. T., Taib, S., Hashim, R., Abidin, M. H. Z., & Rahman, N. I. (2013). Assessment of seawater intrusion to the agricultural sustainability at the coastal area of Carey Island, Selangor, Malaysia. *Arabian Journal of Geosciences, 6*(10), 3909–3928.

Balkaya, Ç., Kaya, M. A., & Göktürkler, G. (2009). Delineation of shallow resistivity structure in the city of Burdur, SW Turkey by vertical electrical sounding measurements. *Environmental Geology, 57*, 571–581. https://doi.org/10.1007/s00254-008-1326-9.

Barnes, G. (2016). *Soil mechanics: principles and practice* (4th ed.). Palgrave, Macmillan Education.

Black, C. A. (1965). Methods of soil analysis, Part 1: Physical and mineralogical properties. The American Society of Agronomy, No. 9, Madison, Wisconsin, USA

Brennan, R. B., Healy, M. G., Morrison, L., Hynes, S., Norton, D., & Clifford, E. (2016). Management of landfill leachate: The legacy of European Union Directives. *Waste Management, 55*, 355–363.

Chiemchaisri, C., Juanga, J. P., & Visvanathan, C. (2007). Municipal solid waste management in Thailand and disposal emission inventory. *Environment Monitoring Assessment, 135*, 13–20. https://doi.org/10.1007/s10661-007-9707-1.

Clarke, B. O., Anumol, T., Barlaz, M., & Snyder, S. A. (2015). Investigating landfill leachate as a source of trace organic pollutants. *Chemosphere, 127*, 269–275.

Göktürkler, G., Balkaya, Ç., Erhan, Z., & Yurdaku, A. (2008). Investigation of a shallow alluvial aquifer using geoelectrical methods: a case from Turkey. *Environmental Geology, 54*, 1283–1290. https://doi.org/10.1007/s00254-007-0911-7.

Haihai, Z., Shaohui, X., Maosheng, G., Jia, Z., Guohua, H., Sen, L., & Xueyong, H. (2018). Heavy metal pollution characteristics in the modern sedimentary environment of Northern Jiaozhou Bay, China. *Bulletin of Environmental Contamination and Toxicology, 101*, 473–478. https://doi.org/10.1007/s00128-018-2439-9.

Haque, M. A., Jahiruddin, M., & Clarke, D. (2018). Effect of plastic mulch on crop yield and land degradation in south coastal saline soils of Bangladesh. *International Soil and Water Conservation Research, 6*(4), 317–324.

Islami, N. (2010). Geoelectrical resistivity and hydrogeochemical contrast between the area that has been applied with fertilization for long duration and non-fertilization. *Journal of Engineering and Technological Sciences, 42*(2), 151–164.

Islami, N., Taib, S., Yusoff, I., & Ghani, A. A. (2011). Time lapse chemical fertilizer monitoring in agriculture sandy soil. *International Journal of Environmental Science & Technology, 8*(4), 765–780.

Islami, N., Taib, S., Yusoff, I., & Ghani, A. A. (2012). Integrated geoelectrical resistivity, hydrochemical and soil property analysis methods to study shallow groundwater in the agriculture area, Machang, Malaysia. *Environmental Earth Sciences, 65*(3), 699–712.

Islami, N., Taib, S., Yusoff, I., & Ghani, A. A. (2018). Integrated geoelectrical resistivity and hydrogeochemical methods for delineating and mapping heavy metal zone in aquifer system. *Environmental Earth Sciences, 77*(10), 383.

Kaya, M. A., Özürlan, G., & Balkaya, Ç. (2015). Geoelectrical investigation of seawater intrusion in the coastal urban area of Çanakkale, NW Turkey. *Environmental Earth Sciences, 73*(3), 1151–1160. https://doi.org/10.1007/s12665-014-3467-3.

Loke, M.H. (2000). Topographic modelling in resistivity imaging inversion. 62nd EAGE Conference & Technical Exhibition Extended Abstracts, D-2.

Loke, M. H. (2004). *Tutorial: 2-D and 3-D electrical imaging surveys, GEOTOMO SOFTWARE, Malaysia*. Etrieved from www.geoelectrical.com

Loke, M. H., & Barker, R. D. (1996). Rapid least-squares inversion of apparent resistivity pseudosections using a quasi-Newton method. *Geophysical Prospecting, 44*, 131–152.

Mor, S., Negi, P., & Khaiwal, R. (2018). Assessment of groundwater pollution by landfills in India using leachate pollution index and estimation of error. *Environmental Nanotechnology, Monitoring & Management, 10*, 467–476.

Negi, P., Mor, S., & Ravindra, K. (2018). Impact of landfill leachate on the groundwater quality in three cities of North India and health risk assessment. *Environment, Development and Sustainability, 22*, 1455–1474. https://doi.org/10.1007/s10668-018-0257-1.

Roger, T., Eubank, A., & Makki, K. (1981). Structural geology of the central Sumatra Back-Arc Basin. *10th Annual Convention Proceedings* 153-196.

Rotich, K. H., Zhao, Y., & Dong, J. (2006). Municipal solid waste management challenges in developing countries – Kenyan case study. *Waste Management, 26*(1), 92–100.

Samadder, S. R., Prabhakar, R., Khan, D., Kishan, D., & Chauhan, M. S. (2017). Analysis of the contaminants released from municipal solid waste landfill site: A case study. *Science of the Total Environment, 580*, 593–601.

Telford, W. M., Geldart, L. P., & Sheriff, R. E. (1990). *Applied Geophysics, 2nd Edition*. Cambridge University.

Thitame, S. N., Pondhe, G. M., & Meshram, D. C. (2010). Characterisation and composition of Municipal Solid Waste (MSW) generated in Sangamner City, District Ahmednagar, Maharashtra, India. *Environment Monitoring Assessment, 170*, 1–5. https://doi.org/10.1007/s10661-009-1209-x.

Ustaoğlu, F., & Tepe, Y. (2018). Water quality and sediment contamination assessment of Pazarsuyu Stream, Turkey using multivariate statistical methods and pollution indicators. *International Soil and Water Conservation Research, In press, 7*, 47–56. https://doi.org/10.1016/j.iswcr.2018.09.001.

Wakode, H. B., Baier, K., Jha, R., & Azzam, R. (2018). Impact of urbanization on groundwater recharge and urban water balance for the city of Hyderabad, India. *International Soil and Water Conservation Research, 6*(1), 51–62.

WHO. (1996). Total dissolved solids in drinking-water: background document for development of WHO Guidelines for Drinking-water Quality. Guidelines for drinking-water quality, 2nd ed. Vol. 2. Health criteria and other supporting information. World Health Organization, Geneva, 1996. Retrieved from https://www.who.int/water_sanitation_health/dwq/chemicals/tds.pdf

Yunmei, W., Jingyuan, L., Dezhi, S., Guotao, L., & Takayuki, S. (2017). Environmental challenges impeding the composting of biodegradable municipal solid waste: A critical review. *Resources, Conservation and Recycling, 122*, 51–65.